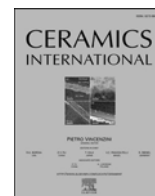




Contents lists available at ScienceDirect

Ceramics International

journal homepage: www.elsevier.com/locate/ceramint

Short communication

Cation-driven electrical conductivity in Ta-doped orthorhombic zirconia ceramics

Bibi Malmal Moshtaghioun^{a,*}, Miguel A. Laguna-Bercero^b, Jose I. Peña^b, Diego Gómez-García^a, Arturo Domínguez-Rodríguez^a^a Departamento de Física de La Materia Condensada, Instituto de Ciencia de Materiales de Sevilla, CSIC-Universidad de Sevilla, PO Box 1065, 41080, Sevilla, Spain^b Instituto de Ciencia de Materiales de Aragón, CSIC-Universidad de Zaragoza, Campus Río Ebro, Sede Campus Río Ebro, Edificio Torres Quevedo, 50018, Zaragoza, Spain

ARTICLE INFO

Keywords:

Tantalum-doped zirconia
Spark plasma sintering
Cationic conductivity

ABSTRACT

This paper is devoted to the study of the electrical conductivity of tantalum-doped zirconia ceramics prepared by spark plasma sintering. In this study, the temperature dependence of conductivity in as-prepared specimens and in those previously annealed in air is determined and compared. A semi-empirical model, which is based on the oxidation states of the cations, has been developed and successfully assessed. According to this, the conductivity is basically controlled by the diffusion of tetravalent zirconium cations in both cases, although the concentration of these species varies drastically with the amount of induced oxygen vacancies. This is a quite unexpected fact, since conductivity is normally controlled by anionic diffusion in zirconia ceramics. This option is forbidden here due to the presence of substitutional pentavalent cations. Therefore, conductivity values are much lower than those reported in trivalent or divalent substitutional cation doped zirconia ceramics.

1. Introduction

Zirconia ceramics are among the most prominent engineering ceramics. This is due to their good structural properties together with excellent electrical conductivity when doped with aliovalent cations such as Mg²⁺, Ca²⁺ or particularly Y³⁺ [1]. The reason for the enhanced ionic conductivity is explained in terms of the increase of anion vacancies produced by the substitutional bivalent or trivalent cations in the cation sub-lattice for electric charge compensation [2]. The applicability of this system relies on excellent structural integrity as well as preservation of the good electrical conductivity. As a consequence of their high oxygen ion conduction, these phases are being widely used in solid oxide fuel cells [3], high temperature electrolysers [4], gas sensors and also in the field of electrocatalysis as an electrolytic support in catalytic applications [5].

In the hope that doping with pentavalent cations would allow the meta-stability of the tetragonal phase at low temperatures under several external conditions, such as high stress or chemically aggressive environments, the ceramics community has moved their attention to ZrO₂-M₂O₅ systems [6]. They belong to a domain in which the lack of scientific knowledge is still immense. The most studied system so far is

the Ta doping zirconia (Ta₂O₅-ZrO₂), with controversial conclusions regarding crystallographic aspects and homogeneity range [7–9].

Quite recently, the potential use of spark plasma sintering for the fabrication of fully dense pieces of Ta-doped zirconia (Ta-ZrO₂ from now on) was successfully reported. The specimens were structurally characterized, particularly their crystallography, oxidation states of the cations in the as-prepared specimens and in those annealed in air. The high-temperature plasticity of those samples is extensively discussed in another publication [8].

This manuscript will cover the lack of information regarding the electrical conductivity of the SPS-ed Ta-ZrO₂ and the role played by the air annealing after sintering. The same type of samples prepared before [7] are used in this work. We will try to elucidate the role of Ta oxidation state on the ionic conductivity. It will be emphasized that conductivity is controlled by the cation sub-lattice, a fact which is quite unusual in zirconia-based ceramics.

2. Experimental procedure

The experimental procedure for sample sintering was previously described [7]. For the sake of clarity to the reader, it is important to

* Corresponding author.

E-mail address: mali_moshtagh@us.es (B.M. Moshtaghioun).

<https://doi.org/10.1016/j.ceramint.2020.10.227>

Received 22 September 2020; Received in revised form 28 October 2020; Accepted 30 October 2020

Available online 2 November 2020

0272-8842/© 2020 Published by Elsevier Ltd.

point out some experimental issues which will be necessary for modelling afterwards:

Firstly, the SPS-ed specimens of 16 mol%Ta–ZrO₂ were sintered at 1250 °C for 5 min under 75 MPa external pressure and they turned black in colour. This is a consequence of the electrochemical blackening typically observed in doped-zirconia ceramics, which occurs under high operation DC electric potentials in reducing/inert atmospheres [10], or also during flash sintering [11] or SPS sintering [12]. The oxidation state of tantalum is predominantly Ta⁴⁺ and zirconium is extensively reduced to Zr³⁺, which induced additional oxygen vacancies. This is confirmed by microanalysis of the samples by XPS and XRD, where the amount of oxygen vacancies was ~19%. We will identify them as “black specimens” or “black set” from now on. Oxygen vacancies compensate the effective negative charge of the Zr³⁺ cations, i.e. there is one oxygen vacancy per two cations.

Secondly, several SPS-ed specimens were annealed in air at 1100 °C for 12 h. These annealed samples turn to get white in colour, a fact which is clearly associated to the elimination of oxygen vacancies, i.e., increase of the oxidation state of the cations. Indeed, XPS results show that the vast majority of tantalum and zirconium are present in the forms Ta⁵⁺ and Zr⁴⁺ respectively. We will call them as “white specimens” or “white set” in what follows. Zr³⁺ cations compensate the positive charge of Ta⁵⁺ ones, i.e. there is one Zr³⁺ cation per Ta⁵⁺ one.

Assuming these facts, we have measured the temperature dependence of DC and AC conductivity. DC electrical conductivity measurements were performed using the four-probe method from room temperature (RT) up to 910 °C using a heating/cooling rate of 2 °C/min. Specimens were placed into a ProboStat™ cell in order to perform the electrical measurements. A current of ±100 mA was applied while the voltage was monitored. Impedance spectroscopy measurements were performed on pellets of 10 mm in diameter and 1 mm in thickness. Platinum electrodes were applied using Pt/Ag paste (ESL9513, Electro Science) deposited on both sides of the pellet, followed by firing at 900 °C for 1 h. Measurements were performed under argon atmosphere for the non-annealed sample and under oxygen atmosphere for the annealed sample. A sinusoidal amplitude of 50 mV was applied, and the frequency was varied from 500 kHz down to 1 Hz. Samples were firstly heated up to 900 °C and then measured down to 600 °C at intervals of about 40 °C. Samples were left for about 1 h to assure temperature stabilization.

Microstructural analyses were performed on polished surfaces by scanning electron microscopy (HITACHI S5200, Japan). The grain size was determined from the SEM pictures. The polished surfaces were thermally etched.

3. Results and discussion

Fig. 1 (a) and (b) show scanning-electron microscopy images of the polished surface of the SPS-ed Ta–ZrO₂ ceramic and after air annealing, respectively. It can be observed that they are dense since essentially there are no pores. Grain size distributions fit to lognormal fitting with a mean grain size ~250 nm in both cases.

Regarding conductivity, the frequency response showed that resistance values are independent of the frequencies at about 1 Hz. Therefore, these values were taken as the resistance of the samples. The electrical conductivity versus the temperature ranged from 600 °C to 910 °C is plotted in Fig. 2 for both samples. Arrhenius-type dependences fit both sets of data, presenting significantly different activation energies: air-treated specimens (white sample) give a value of 1.61 eV, whereas the activation energy for the black sample is much smaller: 0.93 eV. Surprisingly, both conductivities do not numerically differ each other. Even more, they are essentially the same when the temperature is approximately T* = 980 K. At temperatures lower than T*, the conductivity in black specimens is higher, and the opposite takes place in the high-temperature range, i.e. values higher than T*.

This figure is quite remarkable and intriguing. At first sight, a

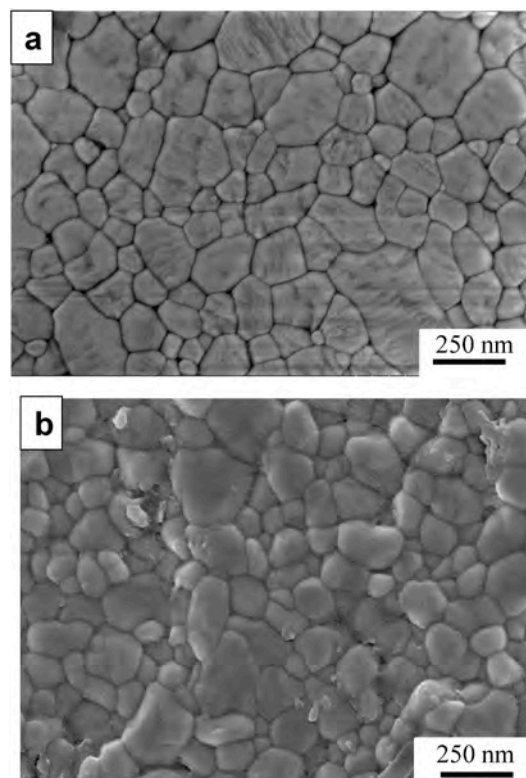


Fig. 1. Scanning electron microscopy micrographs of Ta–ZrO₂ (a) the SPS-ed specimen and (b) after air annealing. The aspect ratio and mean grain size is essentially the same for both sets of specimens.

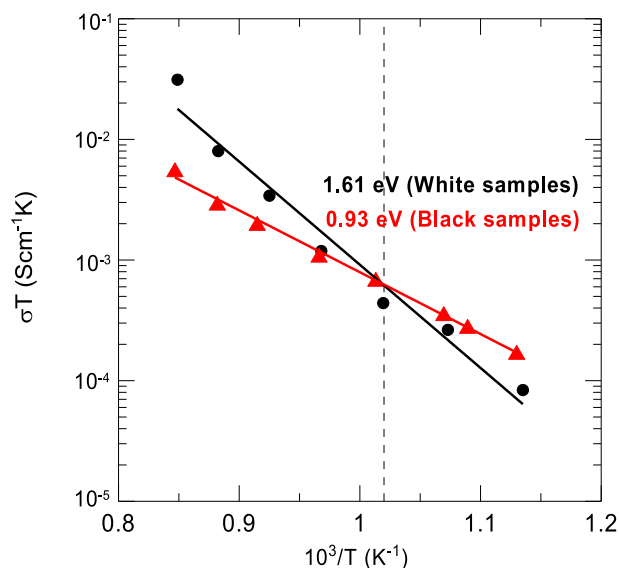


Fig. 2. Temperature dependence of the electrical conductivity for white (air annealed) and black (as SPS-ed) specimens. Both sets of data fit to Arrhenius plots within the temperature range of the experimental set-up. The activation energies are significantly different: 1.61 eV for white specimens compared with 0.93 eV for the black ones. The temperature of iso-conductivity is indicated with a dashed vertical line.

classical explanation in terms of oxygen vacancies-driven conductivity may be the first try. To put into few words, the data fits into Arrhenius plots with activation energies which are in the order of those for oxygen diffusion in other zirconia systems.

However, there is a deep inconsistency which has not been

considered and it makes this system quite singular. If oxygen vacancies were responsible for the conductivity, the values for the black samples necessarily should be much higher than those of the white ones at any temperature. This is because oxygen vacancies are certainly present in the black specimens whereas they are virtually absent in the white ones.

Explanation is subtler, and it requires a deeper insight into the oxidation-reduction processes of the different species into play.

Let us assume that oxygen vacancies are not involved into the electrical conductivity, as they are probably accumulated near the surface. This seems quite surprising at first sight: from a purely theoretical point of view, the contribution of oxygen vacancies to the conductivity should not be discarded. However, in this case this contribution seems to be extremely low according to the experimental pieces of evidence. Indeed, if there were a contribution of oxygen vacancies, that would reach a maximum value in black samples at high temperatures. At this temperature range, the conductivity of black specimens would be much higher than those of white ones. This is contrary to the experimental facts.

At this regard, it is important to emphasize that the value of the conductivity of one chemical species does not depend on the activation energy only. It is also critical the probability of jump to a neighboring position. In this special case, the formation of oxygen vacancies is not favored and very probably they will be partially blocked by the presence of Zr^{3+} , which has an effective negative charge. In the case, the frequency of jumps would be quite small.

Therefore, Zr^{4+} species are the main responsible for conductivity. This is consistent if we consider that Zr^{3+} is species playing a role for charge compensation. Therefore, they are probably associated to positive species such as Ta^{5+} in white samples or oxygen vacancies in black ones. In consequence, their mobility must be much smaller compared with the case of Zr^{4+} ones. We will prove that no other assumption can account for the experimental facts later. The reader must be aware that Zr^{4+} diffusion is equivalent to the motion of Zr^{4+} vacancies, because the formation of interstitials of Zr^{4+} is very unlikely. The concentration of Zr^{4+} vacancies is obviously proportional to the amount of Zr^{4+} cations. The Arrhenius term with the enthalpy of formation is included in the corresponding diffusion coefficient of Zr^{4+} : D_{Zr} [13].

Under these assumptions, the electrical conductivity in white and black doped ZrO_2 samples must follow the Nernst-Einstein [14] equation and it would be given by the following expressions:

$$\sigma_{white} = \frac{N_C}{\Omega} q^2 (x_z - x_3) \frac{D_{Zr}}{kT} = \frac{N_C}{\Omega} q^2 (x_z - x_T) \frac{D_{Zr}}{kT} \quad (1a)$$

$$\sigma_{black} = \frac{N_C}{\Omega} q^2 (x_z - x'_3) \frac{D_{Zr}}{kT} = \frac{N_C}{\Omega} q^2 \left(x_z - 2 \frac{N_o x_o}{N_C} \right) \frac{D_{Zr}}{kT} \quad (1b)$$

For the sake of simplicity, the meaning of all the mathematical symbols used in this work are ordered and collected in Table 1.

The condition of electroneutrality in black specimens has been used in Eq. (1b). In other words, the electric charge of the Zr^{3+} cations per unit cell, which is given by $N_C x'_3 / \Omega$, is compensated by the oxygen vacancies present in one unit cell, i.e. $N_o x_o / \Omega$. In other words:

$$\frac{N_C}{\Omega} x'_3 = 2 \frac{N_o}{\Omega} x_o \quad (2)$$

A straightforward algebra with Eqs (1a) and (1b) allows obtaining the following relationship:

$$\frac{\sigma_{white}}{\sigma_{black}} = 1 + \frac{2 \frac{N_o}{N_C} x_o - x_T}{x_z - 2 \frac{N_o}{N_C} x_o} \quad (3)$$

This equation has strict implications. At sufficiently low temperatures, the concentration of oxygen vacancies is low enough to ensure that $2N_o x_o / N_C < x_T$. When it happens, Eq. (1) predicts that $\sigma_{white} < \sigma_{black}$. On the contrary, at high temperatures: $2N_o x_o / N_C > x_T$, therefore $\sigma_{white} > \sigma_{black}$. There is one temperature at which both conductivities are the

Table 1

Glossary of the symbols used in the model developed in this work.

Mathematical symbols	Meaning
Ω	Volume of the unit cell
N_C	Number of cations per unit cell
N_o	Number of oxygen anions per unit cell
x_z	Fraction of zirconium cations in the unit cell
x_T	Fraction of Tantalum cations per unit cell
x_3	Fraction of Zr^{3+} cations per unit cell in white samples
x'_3	Fraction of Zr^{3+} cations per unit cell in black samples
x_o	Fraction of oxygen vacancies per unit cell in the oxygen sublattice
q	Charge of Zr^{4+} cations
D_{Zr}	Diffusion coefficient of Zr^{4+} cations
Q_{Zr}	Activation energy of the D_{Zr} diffusion coefficient
Q_o	Formation enthalpy of oxygen vacancies
β	$1/kT$. T the absolute temperature and k the Boltzmann constant
σ_{white}	Electrical conductivity in white specimens
σ_{black}	Electrical conductivity in black specimens

same. We will call this the temperature of isoconductivity. Obviously, the condition for isoconductivity is given by:

$$2 \frac{N_o}{N_C} x_o(T^*) = x_T \quad (4)$$

The behaviour derived from Eq. (3) is qualitatively in agreement with the experimental tendency if we consider the temperature $T^* = 980$ K as the frontier between both temperature ranges.

Assuming the usual exponential law for the temperature dependence of oxygen vacancies, a simple calculation in Eq. (4) provides an activation energy which results to be $Q_o \cong 0.25$ eV. This quantity seems to be rather low if compared with the usual values for the activation energy measured in yttria-zirconia, for instance, around 3–4 times higher. This must be intrinsically related to the energy bonding and the singular crystallography of this system, a crystallographic structure which is unique in zirconia systems and have an intense intrinsic polarization [9]. The orthorhombic structure of this system displays a large ferroelectric response.

The value of the activation energy can be confirmed experimentally: the molar concentration of oxygen vacancies of the black samples at 1250 °C, the SPS sintering temperature, was measured by XPS and it is reported to be equal to 0.19 [6]. Assuming the classical exponential dependence for the temperature dependence of the concentration of oxygen vacancies, the activation energy must be $Q_o \cong 0.22$ eV, in good agreement with the previous independent calculation.

Regarding the activation energy, this model can explain the lower activation energy measured in the black specimens. In effect, making use of Eq. (1b) and assuming again an exponential dependence for the temperature dependence of the oxygen vacancies, the activation energy can be calculated in a straightforward way:

$$Q'_{air} = - \frac{\partial \ln \sigma_{white} T}{\partial \beta} = Q_{Zr} \quad (5a)$$

$$Q'_{black} = - \frac{\partial \ln \sigma_{black} T}{\partial \beta} = Q_{Zr} - \frac{2N_o x_o / N_C x_z}{1 - 2N_o x_o / N_C x_z} Q_o = Q_{Zr} - \frac{f}{1-f} Q_o \quad (5b)$$

Where f is the ratio $[Zr^{3+}] / ([Zr^{3+}] + [Zr^{4+}])$. Since the molar concentration of oxygen vacancies is 0.19, the ratio can be calculated easily, and it must give $f \cong 0.76$. Accordingly, the value of Q' is $Q' \cong 0.91$ eV, in good agreement with the experimental outputs.

The reader could imagine that other options might account for these experimental outputs. In particular, the option of Zr^{3+} to be responsible for the electrical conductivity could be proposed at first sight. However, a simple inspection reveals that this approach must be discarded: in white specimens the concentration of Zr^{3+} cations is imposed by the

concentration of Ta⁵⁺ ones. Thus, this value being constant, the activation energy for electrical conductivity would be that of the diffusion coefficient for Zr³⁺. On the contrary, in black specimens, the concentration of Zr³⁺ cations are imposed by the oxygen vacancies concentration. Since this one increases with temperature, the activation energy should be much higher: the sum of that for Zr³⁺ diffusion plus the contribution of Q₀. But this is against the experimental facts.

No other option can explain the experimental results to the best of the authors' knowledge.

Additional analysis of the EIS measurements was performed. As an example, Nyquist plots recorded at OCV at 860 °C and 660 °C for both samples are shown. A simple equivalent electrical circuit composed of a resistance (R) in parallel with a constant phase element (CPE) was used to fit the experimental data. A summary of the fitting parameters is also given in Tables 2 and 3. In terms of total conductivity, these results are in concordance with the electrical conductivity switch for both samples, as it was discussed and observed in Fig. 2.

In a typical good ionic conductor such as YSZ (yttria stabilized zirconia), the impedance spectra exhibited two semi-circles attributed to both bulk grains and grain boundaries. The semi-circle at high frequencies corresponds to the bulk and the low frequency contribution corresponds to the resistance through grain boundaries. In addition, samples fabricated by SPS significantly reduce the contribution of grain boundary resistivity in comparison with conventional sintering. This finding was observed for the YSZ case, where the maximum ionic conductivity of SPS sample could be enhanced by 50% in comparison with a conventionally sintered sample [12].

According to the well-known impedance analysis for distinguishing grain/bulk or grain boundaries in ceramics, the typical capacitance values of the responses for the bulk and grain boundary response are in the range of 10⁻¹² F/cm² and 10⁻⁸ F/cm², respectively [15]. However, in our case only one R-CPE element was observed. This can be related with the crystal structure. For the Ta-doped ZrO₂ samples, although the main structure is orthorhombic, it was previously reported that the Ta-doped ZrO₂ sample also presents partial transformation from the orthorhombic to the monoclinic polymorph [7]. Furthermore, the precipitation of the monoclinic polymorph could explain the absence of vacancies, induced by the corresponding changes in structural disorder and local strains. Then, it is reasonable to assume that the conductivity behaviour could be comparable to that of monoclinic ZrO₂ [16].

As observed in Table 2, the obtained capacitance values are in the range of 10⁻¹⁰ F/cm² which are consistent with the bulk (gran interior) [17]. This is also consistent with the results of Kwon et al. for monoclinic zirconia [16], despite the considerable resistance expected due to the large portion of grain boundaries in samples with ~250 nm grains. This

Table 2

Experimental results of the resistance, specific capacitance, frequency of the sinusoidal signal applied in the sample, resistivity and conductivity for the SPS-ed as prepared specimens (black ones).

Temperature (°C)	R (kΩ)	C (Fcm ⁻²)	ν (Hz)	Resistivity (Ωcm)	Conductivity (Scm ⁻¹)
908	28.1	4.41 × 10 ⁻¹⁰	12,843	2.11 × 10 ⁵	4.74 × 10 ⁻⁶
861	51.0	5.15 × 10 ⁻¹⁰	6068	3.83 × 10 ⁵	2.61 × 10 ⁻⁶
820	72.1	5.01 × 10 ⁻¹⁰	4408	5.42 × 10 ⁵	1.84 × 10 ⁻⁶
762	125.4	4.82 × 10 ⁻¹⁰	2631	9.43 × 10 ⁵	1.06 × 10 ⁻⁶
714	189.6	4.88 × 10 ⁻¹⁰	1718	1.42 × 10 ⁶	7.01 × 10 ⁻⁷
662	346.0	5.20 × 10 ⁻¹⁰	884	2.60 × 10 ⁶	3.84 × 10 ⁻⁷
645	433.8	4.95 × 10 ⁻¹⁰	740	3.26 × 10 ⁶	3.07 × 10 ⁻⁷
612	685.0	4.85 × 10 ⁻¹⁰	478	5.15 × 10 ⁶	1.94 × 10 ⁻⁷

Table 3

Experimental results of the resistance, specific capacitance, frequency of applied the sinusoidal signal, resistivity and conductivity for the SPS-ed and ulterior air annealing samples (white ones).

Temperature (°C)	R (kΩ)	C (Fcm ⁻²)	ν (Hz)	Resistivity (Ωcm)	Conductivity (Scm ⁻¹)
905	552.8	8.33 × 10 ⁻¹⁰	34,551	3.77 × 10 ⁴	2.65 × 10 ⁻⁵
860	207.7	6.38 × 10 ⁻¹⁰	12,001	1.42 × 10 ⁵	7.05 × 10 ⁻⁶
808	463.5	8.62 × 10 ⁻¹⁰	3981	3.16 × 10 ⁵	3.16 × 10 ⁻⁶
760	127.1	6.45 × 10 ⁻¹⁰	1940	8.68 × 10 ⁵	1.15 × 10 ⁻⁶
708	326.4	7.32 × 10 ⁻¹⁰	666	2.23 × 10 ⁶	4.48 × 10 ⁻⁷
659	516.5	6.76 × 10 ⁻¹⁰	455	3.52 × 10 ⁶	3.84 × 10 ⁻⁷
608	1620	7.16 × 10 ⁻¹⁰	137	1.10 × 10 ⁶	9.04 × 10 ⁻⁸

is also consistent with the oxygen vacancy model, explaining the effect of the dopant content on the electrical conductivity. Fig. 3 displays the Cole-Cole plots at two different temperatures values for both types of specimens. The absence of a second semi-circle suggests that grain boundaries present no diffusion paths through the grain interior, as oxygen vacancy depletion regions are associated with grain boundaries.

4. Conclusions

A model based on microstructural analysis of the oxidation state of metal cations in Ta-ZrO₂ is proposed. The model can explain the main features of the temperature dependence of the conductivity in SPSed-sintered samples as well as those annealed in air. According to this model, conductivity is controlled by the diffusion of zirconium cations, a fact which is observed for the first time in zirconia-based ceramics. Despite this success, there is a challenging question which deserves

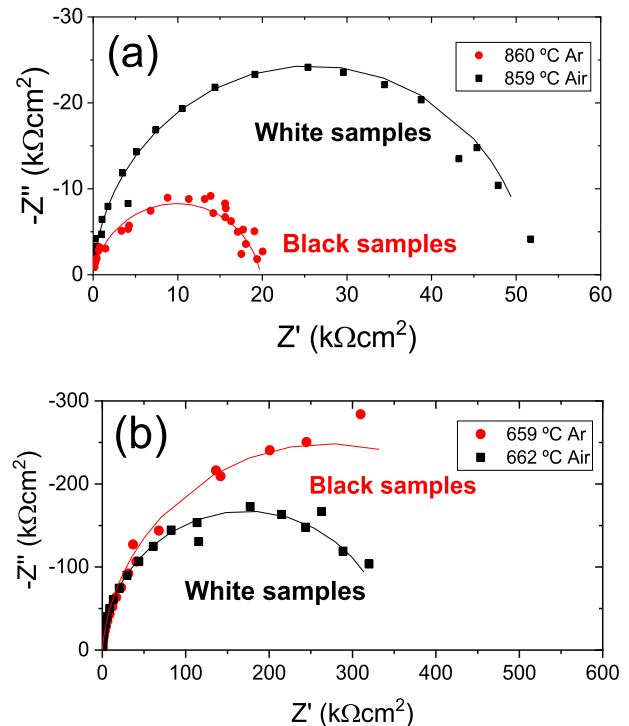


Fig. 3. Cole-Cole plots for both sets of samples at two different temperatures: (a) 860 °C and (b) 660 °C.

much attention: the reason why activation energy for zirconium diffusion reaches values as low as 0.25 eV.

Declaration of competing interest

The authors declare that they have no known competing financial interests or personal relationships that could have appeared to influence the work reported in this paper.

Acknowledgements

The authors would like to acknowledge provided by several institutions:

BMM wants to acknowledge the Spanish Ministry of Science and Innovation through the grant PID2019-103847RJ-I00, as well as the financial support awarded by the Regional government of the 'Junta de Andalucía' through the project P18-RTJ-1972.

BMM and JIP gratefully acknowledge the financial support provided the Ministry of Science in Spain through the projects MAT2016-77769-R and Gobierno de Aragón, Spain (Grupo Reconocido DGA T02_17R) and the associated EU Regional Development Funds. MLB acknowledges the funding support provided by the projects MAT2015-68078-R and PID2019-107106RB-C32 funded by the Spanish Ministry of Science and Innovation.

Finally, DGG and ADR are grateful to the Spanish Ministry of Science for the research funding through the project MAT2015-71411-R.

References

- [1] S. Hui, J. Roller, S. Yick, X. Zhang, C. Decès-Petit, Y. Xie, R. Maric, D. Ghosh, A brief review of the ionic conductivity enhancement for selected oxide electrolytes, *J. Power Sources* 172 (2007) 493–502.
- [2] H.I. Tuller, Chapter 6: mixed conduction in nonstoichiometric oxides, in: O. T. Sørensen (Ed.), *Non-stoichiometric Oxides*, Academic Press, New York, 1981, pp. 271–333.
- [3] N. Mahato, A. Banerjee, A. Gupta, S. Omar, K. Balani, Progress in material selection for solid oxide fuel cell technology: a review, *Prog. Mater. Sci.* 72 (2015) 141–337.
- [4] M.A. Laguna-Bercero, Recent advances in high temperature electrolysis using solid oxide fuel cells: a review, *J. Power Sources* 203 (2012) 4–16.
- [5] M.N. Tsampas, F.M. Sapountzi, P. Vernoux, Applications of yttria stabilized zirconia (YSZ) in catalysis, *Catal. Sci. Technol.* 5 (2015) 4884–4900.
- [6] G. Gritzner, C. Puchner, V2O5, Nb2O5 and Ta2O5 doped zirconia ceramics, *J. Eur. Ceram. Soc.* 13 (5) (1994) 387–394.
- [7] G. Sponchia, B.M. Moshtaghioun, A. Benedetti, P. Riello, D. Gómez-García, A. Domínguez-Rodríguez, A.L. Ortiz, Ceramics of Ta-doping stabilized orthorhombic ZrO₂ densified by spark-plasma sintering and the effect of post-annealing in air, *Scripta Mater.* 130 (2017) 128–132.
- [8] G. Sponchia, B.M. Moshtaghioun, P. Riello, A. Benedetti, D. Gómez-García, A. Domínguez-Rodríguez, A.L. Ortiz, High-temperature compressive creep of novel fine-grained orthorhombic ZrO₂ ceramics stabilized with 12 mol% Ta doping, *J. Eur. Ceram. Soc.* 38 (5) (2018) 2445–2448.
- [9] F.L. Cumbreira, G. Sponchia, A. Benedetti, P. Riello, J.M. Pérez-Mato, A.L. Ortiz, Crystallographic considerations on the novel orthorhombic ZrO₂ stabilized with Ta doping, *Ceram. Int.* 44 (2018) 10362–10366.
- [10] M.A. Laguna-Bercero, V.M. Orera, Micro-spectroscopic study of the degradation of scandia and ceria stabilized zirconia electrolytes in solid oxide electrolysis cells, *Int. J. Hydrogen Energy* 36 (2011) 13051–13058.
- [11] M. Biesuz, L. Pinter, T. Saunders, M. Reece, J. Binner, V.M. Sglavo, S. Grasso, Investigation of electrochemical, optical and thermal effects during flash sintering of 8YSZ, *Materials* 11 (7) (2018) 1214.
- [12] X.J. Chen, K.A. Khor, S.H. Chan, L.G. Yu, Preparation yttria stabilized zirconia electrolyte by spark plasma sintering, *Mater. Sci. Eng., A* 341 (2003) 43–48.
- [13] J.B. Goodenough, in: P. Hagemuller, W. Van Gool (Eds.), *Solid Electrolytes*, Academic Press, New York, 1978, pp. 393–415.
- [14] J.D. Solier, I. Cachadina, A. Domínguez-Rodríguez, Ionic conductivity of ZrO₂ 12 mol%-Y₂O₃ single crystals, *Phys. Rev. B* 48 (6) (1993) 3705–3712.
- [15] J.T.S. Irvine, D.C. Sinclair, A.R. West, Electroceramics: characterization by impedance spectroscopy, *Adv. Mater.* 2 (1990). No. 3.
- [16] O.H. Kwon, C. Jang, J. Lee, H.Y. Jeong, Y. Kwon, J.H. Joo, H. Kim, Investigation of the electrical conductivity of sintered monoclinic zirconia (ZrO₂), *Ceram. Int.* 43 (2017) 8236–8245.
- [17] J. Nielsen, J. Hjelm, Impedance of SOFC electrodes: a review and a comprehensive case study on the impedance of LSM: YSZ cathodes, *Electrochim. Acta* 115 (2014) 31–45.